

Hybrid Artifact Detection System for Minute Resolution Blood Pressure Signals from ICU

Hollan Haule
School of Engineering, IDCOM
University of Edinburgh
Edinburgh, UK
0000-0003-3691-3816

Evangelos Kafantaris
School of Engineering, IDCOM
University of Edinburgh
Edinburgh, UK
0000-0001-9599-7656

Tsz-Yan Milly Lo
Centre of Medical Informatics, Usher Institute
University of Edinburgh
Edinburgh, UK
mils.lo@ed.ac.uk

Chen Qin
School of Engineering, IDCOM
University of Edinburgh
Edinburgh, UK
0000-0003-3417-3092

Javier Escudero
School of Engineering, IDCOM
University of Edinburgh
Edinburgh, UK
0000-0002-2105-8725

Abstract—Physiological monitoring in intensive care units generates data that can be used to aid clinical decision making facilitating early interventions. However, the low data quality of physiological signals due to the recording conditions in clinical settings limits the automated extraction of relevant information and leads to significant numbers of false alarms. This paper investigates the utilization of a hybrid artifact detection system that combines a Variational Autoencoder with a statistical detection component for the labeling of artifactual samples to automate the costly process of cleaning physiological recordings. The system is applied to mean blood pressure signals from an intensive care unit dataset recorded within the scope of the KidsBrainIT project. Its performance is benchmarked to manual annotations made by trained researchers. Our preliminary results indicate that the system is capable of consistently achieving sensitivity and specificity levels that surpass 90%. Thus, it provides an initial foundation that can be expanded upon to partially automate data cleaning in offline applications and reduce false alarms in online applications.

Index Terms—Data quality, physiological signals, artifact detection, autoencoders, variational autoencoders

I. INTRODUCTION

Beside physiological monitoring of critically ill patients in the Intensive Care Units (ICU) generates wealth of data. The effective utilization of these data can lead to early and personalized disease interventions. In the case of Traumatic Brain Injury (TBI), real-time monitoring is crucial for early detection and prevention of secondary insults [1]. TBI accounts for the majority of injury-related deaths in Europe [2]. Worldwide, it is estimated that 50 million TBI cases occur annually [3]. Given this burden, it is essential to develop procedures to improve the clinical management of TBI patients.

Typically, ICU patient monitoring involves collection of continuous recording of patients' physiological state signals

This research was funded in part by an EPSRC Doctoral Training Partnership PhD studentship and The Carnegie Trust for the Universities of Scotland (RIG009251). For the purpose of open access, the author has applied a Creative Commons Attribution (CC BY) licence to any Author Accepted Manuscript version arising from this submission.

such as blood pressure, core temperature, and blood gas levels [4]. However, the intrinsic conditions of clinical work in the ICU lead to significantly low-data quality. Patient movement, probe change, position change, and accidental dislodgement of probes lead to discontinuous recordings [5]. Procedures such as arterial blood sampling may also lead to absence of reliable readings for a short period of time.

Senior clinicians are trained to ignore artefacts in their clinical decision making. However, outliers and low data quality can still trigger alarms in the monitoring devices, potentially resulting in “alarm fatigue” [5], where clinical staff could ignore alarms which they perceive as false, even when they could be accurate, due to the extensive number of false positive alarms occurring from artifactual signal segments. Furthermore, any utilization of raw ICU data for offline clinical research is also limited due to the low-data quality. Currently, the “gold standard” for removing artifacts is manual annotation by experienced researchers, which is time-consuming and biased due to inter-observer variability [6].

A number of techniques have been used to detect artifacts in high frequency physiological data. In [5], it is highlighted that Signal Quality Indices (SQIs), which are hand-crafted features derived to measure the quality of a signal, are popular techniques for detecting artifacts in ICU. However, most SQIs detect artifacts in high-frequency waveform data [7]. Signal abnormality index (SAI) is an example of algorithms for detecting artifacts in arterial blood pressure waveform [8]. In [9], a convolutional variational autoencoder (VAE) was used to detect artifacts in arterial blood pressure waveform, showing that the model outperforms Principal Component Analysis (PCA) algorithm. However, the work is based on one patient's data and remains to be tested in patient agnostic applications. Similarly, in [10], a Deep Belief Network (DBN) was also used to detect and eliminate artifacts in high-frequency blood pressure waveform signals. Moving closer to clinical application, there is growing interest in utilizing

minute-by-minute data, due to the higher availability of in ICU environment [11]. Therefore, developing techniques for detecting artifacts in low frequency ICU data would facilitate this research. Furthermore, the successful implementation of a system for the analysis of low temporal resolution data could potentially indicate its implementability for the analysis of higher resolution data, since a more accurate representation of physiological dynamics is available in that case, making the detection of artifacts easier [12].

As an initial step in addressing this challenge, we propose an automated artifact detection system for minute-by-minute physiological recordings from ICU based on the combination of a VAE and a statistical component. We compare the performance of our proposed system with one employing a vanilla autoencoder (AE) and the statistical component. We also assess the impact of the threshold to detect artifacts and the regularisation in the VAE in the results. The (V)AE-based component is tested in multiple configurations using autoencoder (AE) and (VAE) configurations built with LSTMs focusing on the detection of “spike” errors which consist of commonly recorded outliers that can overshadow physiological dynamics by disrupting the patterns of the recorded signal. The statistical detection component focuses on the detection of “flatline” errors that occur during the disconnection of monitoring equipment from patients. The performance of the system is tested through its application to mean blood pressure signals (Bpm) extracted from an ICU dataset that has been annotated by an expert researcher with over 30 years of experience and contains recordings with low temporal resolution similar to the majority of clinical datasets that can be extracted from ICU as opposed to the high temporal resolution datasets that have been the main focus of previous research [7], [9], [10].

II. MATERIALS AND METHODS

A. Dataset description

This study utilizes the dataset from the KidsBrainIT project, that was collected prospectively and extracted for research purposes after the patient is discharged from Paediatric intensive care units (PICU). This is multi-centre, multi-disciplinary, multi-national dataset of patients selected from 16 PICU in 7 countries [13]. This includes 125 patients aged ≥ 14 . From each patient, ≤ 14 physiological signals were collected at minute-by-minute intervals by a data acquisition system (*Edinburgh Monitor*[®]) and annotated by an experienced clinician using (*Edinburgh Browser*[®]), a data validating and analysing system [1]. The analysis presented in this study is applied to the Bpm time-series of each selected record.

B. Data preprocessing

From the 125 patient files included in the original dataset, 85 are selected based on the availability of Bpm recordings that contain at least 90% of numerical data for the entire length of each recording. Numerical data is considered any sample point, physiological or artifactual, that is not signified in the recording as not a number. Consequently “flatline” errors are also considered as numerical data during this selection process

as they cannot be distinguished just with their initial format. The selection is made to exclude patient records that either did not contain any recording of Bpm or contained extensively large sections of missing Bpm data. The selected records are then split in 53 patient records for training, 15 patient records for validation and 17 patient records for testing. The selection of records for each set is done at random.

For each patient’s record separately, Bpm is scaled by subtracting the median and then dividing by the Interquartile range ($75^{\text{th}} - 25^{\text{th}}$). The scaling is applied at the record level to ensure that differences in the blood pressure range of each patient are preserved when training the AE and VAE while reducing the effect of outliers. Each record within the training set is split in overlapping windows of 60 minutes corresponding to 60 samples in length (W) with a sliding window step size of 1 minute. The window length is selected to allow the analysis of even short-term recordings, with the minimum recording length found in the selected records being ≤ 120 minutes, while still maintaining a minimum number of samples for the effective learning of temporal dynamics of the recordings. The small step size and the overlapping of windows allows for improved training of the model [14].

For every record in the training set, the annotated labels are used to identify and remove artifactual samples to ensure that the (V)AE-based component of the system is trained on clean patterns of physiological dynamics as opposed to artifactual ones. The windows of each record are then shuffled and combined to ensure that the training will be done in a patient agnostic manner. This results in a training matrix of windows with dimensions $N \times W$ where $W = 60$ and N is the total number of windows.

C. Artifact Detection System

1) *Statistical Component*: The statistical component has foundations in statistical anomaly detection techniques [15]. Typically, a statistical method involves fitting a model to normal data and then use this model to test if new samples fit in this model. In this study, prior knowledge of “flat-line” artifacts allows us to use a flat line to detect these kinds of artifacts. This component utilizes a small overlapping sliding window with a step size of 1 sample to detect “flatline” signal segments. For each group of samples a line is fit to calculate its gradient (∇) and an artifactual label is attached to the last sample of the group if its value is $|\nabla| < 10^{-9}$ which indicates no fluctuation in the Bpm time-series. For each overlapping window the label of the last sample is the one being labelled as either valid or artifactual. The statistical component of the system is deployed directly on the validation and testing data without any form of interaction with training data.

2) *(V)AE-based Component*: Long Short-Term Memory (LSTM) is a type of recurrent neural network (RNN) capable of learning over long sequential data. A basic LSTM has in addition to a hidden state, memory cells with their own recurrence network, which shares inputs and outputs with the main recurrent network and gates that enable efficient flow of information [16], [17].

The (V)AE-based component consists of an LSTM encoder-decoder architecture. The encoder and decoder consists of two LSTM layers each. Training this component with artifact free data enables this architecture to learn a latent space which considers the temporal physiological dynamics of the signal, as the artefactual segments have been removed from the training dataset. A test sample is then mapped into this space and then reconstructed back. This sample is classified as an artifact if the reconstruction error ($\delta = | \mathbf{x} - \mathbf{x}' |$) is above a certain threshold. This assumption has foundations in Neural Network-based and spectral anomaly detection techniques [15].

An AE is a deep learning architecture for representation learning, utilizing the encoder and decoder format. The encoder maps a data point (\mathbf{x}) to its low dimensional representation (\mathbf{z}), $\mathbf{z} = \text{Encoder}(\mathbf{x})$, and the decoder is a reverse mapping to the original data point, $\mathbf{x}' = \text{Decoder}(\mathbf{z})$ [16]. The complete approximation process is defined as: $\mathbf{x} \simeq \text{Decoder}(\text{Encoder}(\mathbf{x}))$.

An AE learns these mappings by minimizing a reconstruction loss between the actual input, \mathbf{x} , and its reconstruction, \mathbf{x}' . An example of the reconstruction loss is mean squared error. However, unconstrained AEs have a weakness in that they tend not to learn meaningful representations of the data. They learn to copy the input data as-is without learning functional features [16].

Constrained AEs on the other hand, tend to learn meaningful representations by adding a regularization term in the loss function. A VAE [18] is a form of constrained AEs that stems from probabilistic models. It belongs to a group, referred to as Deep Latent Variable Models (DLVM), that uses a neural network to approximate the joint distribution of observed (\mathbf{x}) and latent variables (\mathbf{z}), $p_{\theta}(\mathbf{x}, \mathbf{z})$ [19]. The VAE learns the latent representation of the data by using an encoder, $q_{\phi}(\mathbf{z}|\mathbf{x})$, to approximate a Gaussian posterior distribution $p_{\theta}(\mathbf{z}|\mathbf{x})$. Sampling from this distribution, \mathbf{z} , and feeding them into the decoder, $p_{\theta}(\mathbf{x}|\mathbf{z})$, generates new meaningful samples, \mathbf{x} . The reparameterization step [16], [19] enables the VAE to be trained by gradient backpropagation algorithm. VAEs are trained by maximizing the Evidence Lower Bound (ELBO) shown in the following equation [19].

$$\mathcal{L}(\theta, \phi; \mathbf{x}) = \mathbb{E}_{q_{\phi}(\mathbf{z}|\mathbf{x})} [\log p_{\theta}(\mathbf{x}|\mathbf{z})] - D_{KL}(q_{\phi}(\mathbf{z}|\mathbf{x})||p_{\theta}(\mathbf{z}))$$

This is equivalent to a regularized AE, where the Kullback–Leibler (KL) divergence acts as a regularizer. β -VAE [20] is an extension of the original VAE [18], that introduces a regularization coefficient, β , on the ELBO as shown in the following equation.

$$\mathcal{L}(\theta, \phi; \mathbf{x}) = \mathbb{E}_{q_{\phi}(\mathbf{z}|\mathbf{x})} [\log p_{\theta}(\mathbf{x}|\mathbf{z})] - \beta D_{KL}(q_{\phi}(\mathbf{z}|\mathbf{x})||p_{\theta}(\mathbf{z}))$$

Varying the parameter β encourages the model to learn disentangled representations in the latent space [20]. For example, increasing the value of β leads to loss of higher frequency components [20]. This is an attractive feature in

detecting some types of artifacts, which tend to lie in the high frequency bands, at the cost of poor reconstructions of the signal. However, a balanced β value selection is required to avoid extensive low-pass filtering of the reconstruction.

In this study, we utilize the (V)AE-based component in different configurations of AE and VAE architectures. Across all tested configurations the dimensions of the encoder and decoder are kept the same in a symmetrical setup. The encoder and decoder consist of two LSTM layers, each with the hidden dimension size being 64. The bottleneck dimension size is 12. These dimension sizes are tuned utilizing the validation set of patient records. The deployment of the (V)AE component both on validation and testing sets is done using overlapping windows of 60 samples length with step size of 1 sample similarly to the format followed for the training data.

3) *Detection Merging*: The artifactual label outputs of the statistical and (V)AE-based components are finally merged using an OR logical function where a sample is labelled as artifactual if it has been labelled as such either by one or both of the components.

D. Validation Set Tuning

1) *Statistical Component Tuning*: The 15 patient records in the validation set are used to initially tune the window size of the statistical component. The window sizes of 5, 10 and 15 samples are tested and the performance of the statistical component is measured using the available annotations from the record. The window size of 10 samples is selected to provide an adequate period of time for which the lack of fluctuations in the value of the measured parameter would be abnormal based on *a priori* medical knowledge, as opposed to the 5 sample option, while remaining small enough so that the labelling of potentially valid sample points remains minimal as opposed to the case of 15 samples.

2) *(V)AE Component Tuning*: The validation set is then used for the definition of a β value range of the VAE configurations and a δ threshold percentile (Q) range for both the AE and VAE configurations based on which a sample will be labelled as valid or a "spike" error during the deployment of the (V)AE component.

For β , the value range of 0.1, 0.2, 0.3, 0.4, 0.5, 0.6 is set after analysing the signal reconstructions for VAE configurations trained on the training records and deployed on the validation records. The starting point of 0.1 is selected as a clear separation point from the operation of a traditional AE while the range stops at 0.6 since the bandwidth of the reconstructed signal becomes significantly limited to low frequency fluctuations for $\beta > 0.6$.

For the definition of a Q range each of the seven (V)AE configurations, one for AE and six for VAE, are deployed on the validation set. A δ distribution is constructed per configuration and processed using the statistical component of the system to remove the δ values of samples labelled as "flatline" errors. While the operation of the statistical component is not expected to be perfect, this step ensures that the majority of "flatline" δ values are removed to ensure that the Q range

TABLE I
AUTOENCODER AND VARIATIONAL AUTOENCODER $\beta = 0.1$

Q	Sensitivity AE	Sensitivity VAE	Specificity AE	Specificity VAE
90 th	0.942	0.95	0.835	0.854
92 nd	0.937	0.944	0.857	0.872
94 th	0.929	0.933	0.879	0.889
96 th	0.919	0.923	0.899	0.906
98 th	0.903	0.905	0.921	0.926

selected, is calibrated for the detection of "spike" errors. Based on the resulting δ distributions the Q percentile range of 90th, 92nd, 94th, 96th, 98th with each percentile consisting of an array of seven values that are used in the following testing set experiments, one for each (V)AE configuration.

E. Testing Set Experiments

Using the parameter ranges defined utilizing the validation set, the system is implemented and tested in a total of 35 experimental setups based on all combinations of $\beta + 1$ (including the AE) and Q values. Each experimental setup is repeated for five iterations and the performance of the system is measured through the calculation of the mean and standard deviation (σ) of the sensitivity and specificity metrics. For the calculation of these metrics the following terms are used:

- True Positive (TP): An artifactual sample correctly labelled as artifactual.
- True Negative (TN): A valid sample correctly labelled as valid.
- False Positive (FP): A valid sample incorrectly labelled as artifactual.
- False Negative (FN): An artifactual sample incorrectly labelled as valid.

The performance metrics are calculated as follows:

$$sensitivity = \frac{TP}{TP + FN} \quad specificity = \frac{TN}{TN + FP}.$$

III. RESULTS AND DISCUSSION

All results reported in this section consist of the performance calculated after the merging of the labels provided from the statistical and the (V)AE-based components of the system. Table I displays the mean values of sensitivity and specificity for the artifact detection system while using an AE architecture and VAE with $\beta = 0.1$. Figure 1 displays the mean and σ of the sensitivity calculated from the five iterations for each experimental setup of VAE β and Q , values while the respective values of specificity are plotted in Figure 2. The statistical component remained the same across all experimental setups.

A. AE and VAE Comparison

When comparing the performance of the AE architecture to the VAE architecture with $\beta = 0.1$, the VAE architecture consistently outperforms the AE architecture with regards to both its specificity and sensitivity with the performance increase being higher for specificity. Consequently, we would recommend the utilization of the VAE architecture over AE

since it provides superior performance and increased control of its operation through the selection of the β value.

B. VAE Configurations

The value of the Q parameter controls how strict the threshold becomes for a sample to be labelled as an artifact based on its δ . Higher values such as $Q = 98^{\text{th}}$ correspond to a less strict threshold for the labelling of a sample as an artifact as opposed to lower values such as $Q = 90^{\text{th}}$. As expected, increases in the value of Q lead to higher values of specificity at the cost of reduced sensitivity since for a less strict threshold the number of "spike" errors correctly labelled as artifactual (TP) will be lower but so will the number of valid samples incorrectly labelled as "spikes" (FP). Out of the two parameters tested, Q has the largest effect in the calculated performance metrics.

Increasing the VAE β leads to reconstructions with fewer high frequency components due to the regularization step of VAEs. Consequently, the specificity of the model increases due to a more clear definition between physiological fluctuations and artifactual "spikes". However a drop in sensitivity is also noted since certain "spike" errors can also be "regularized" during the reconstruction. The effect of β is noticeably higher for lower Q values 90th, 92nd with increased β values favouring specificity at the cost of sensitivity as described. At Q values of 96th and 98th changes in β lead to minimal differences on specificity and sensitivity.

Consequently, considering the effects of Q and β parameters and as shown in Figures 1, 2 the highest value of specificity is achieved from the configurations with $Q = 98^{\text{th}}$ while the highest value of sensitivity is achieved from the configuration with $Q = 90^{\text{th}}$, $\beta = 0.1$. Minor overlapping is observed in the values of sensitivity for configurations with $Q = 92^{\text{nd}}$ and 94th at $\beta = 0.4$ across the five experimental iterations while no overlapping is observed for values of specificity. The maximum σ observed across all experimental setups is $4 \cdot 10^{-3}$. Finally, the configurations with $Q = 94^{\text{th}}$, $\beta = 0.6$ and $Q = 96^{\text{th}}$, $\beta = 0.5$ achieve a balanced profile of specificity and sensitivity.

C. Limitations of Study and Future Work

The recorded performance in this preliminary study is the result of the combined output labels of the statistical and the (V)AE-based components of the hybrid detection system. Thus, the differences between the tested configurations can be dampened due to the steady performance of the statistical component that remains the same across all experimental setups. Due to the prevalence of "flatline" errors in respective datasets we consider important the integration of the statistical component. For future studies we would be interested in utilizing an architecture that could detect both "flatline" and "spike" errors using the same component to reduce the complexity of the system.

The presented system was implemented on the BPm time-series of the dataset. However, the available recordings include additional time-series formulated from Intracranial pressure

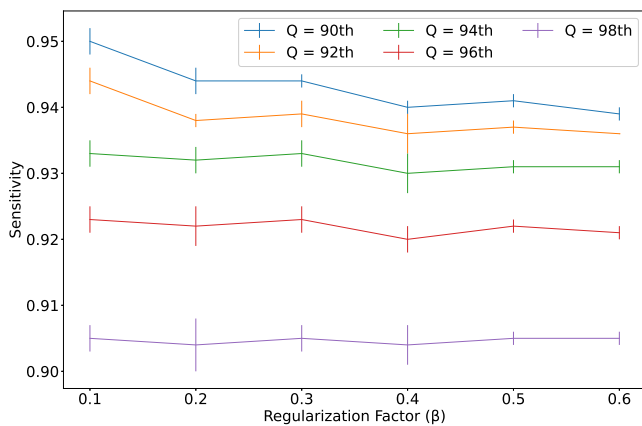


Fig. 1. Mean sensitivity plotted for each combination of VAE: Q and β values.

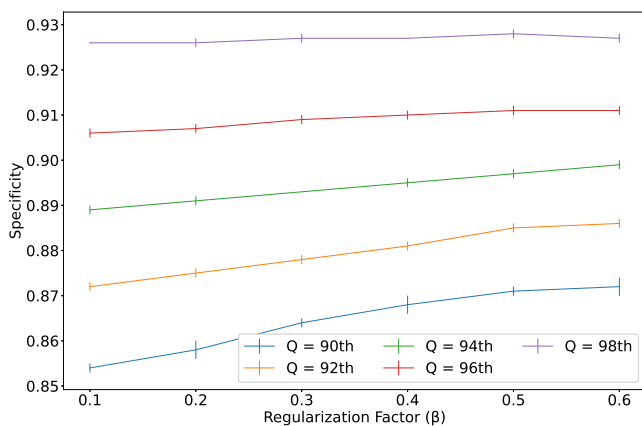


Fig. 2. Mean specificity plotted for each combination of VAE: Q and β values. Points without error bars correspond to $\sigma < 10^{-3}$.

(ICP), respiratory rate (RR) and Oxygen Saturation signals. It would therefore be important to utilize the available time-series to verify the robustness of the approach across different physiological signals and to study the operation of a multivariate (VAE)-based component.

Furthermore, the presented system has been designed to be trained and deployed in an offline manner. However, it provides a foundation that can be expanded upon for online applications through the potential combination of saved offline pre-trained models with shorter online training batches. Finally, the utilization of VAE configurations for unsupervised learning would allow the utilization of the system for the cleaning of datasets that do not contain annotations of artifactual samples that could be used for training.

IV. CONCLUSION

This study reports preliminary results in the deployment of an artifact detection system consisting of a (VAE)-based and a statistical detection component for the detection of "spike" and "flatline" errors in BPM time-series. The presented system is

successful in achieving offline detection of artifactual samples with both sensitivity and specificity values in the $> 90\%$ range. However, future research is required for the optimization of the system, to allow its utilization on datasets that do not contain training labels as well as the development of online training to allow its implementation in clinical environments.

REFERENCES

- [1] P. A. Jones, P. J. Andrews, V. J. Easton, and R. A. Minns, "Traumatic brain injury in childhood: Intensive Care time series data and outcome," *British Journal of Neurosurgery*, vol. 17, no. 1, 2003.
- [2] F. Tagliaferri, C. Compagnone, M. Korsic, F. Servadei, and J. Kraus, "A systematic review of brain injury epidemiology in Europe," 2006.
- [3] F.-t. H. Pdf, "Traumatic brain injury : integrated approaches to improve prevention , clinical care , and research Traumatic brain injury : a global challenge," *The Lancet Neurology*, pp. 3–5, 2020.
- [4] M. D. Sorani, J. C. Hemphill, D. Morabito, G. Rosenthal, and G. T. Manley, "New approaches to physiological informatics in neurocritical care," 2007.
- [5] A. E. Johnson, M. M. Ghassemi, S. Nemati, K. E. Niehaus, D. Clifton, and G. D. Clifford, "Machine Learning and Decision Support in Critical Care," *Proceedings of the IEEE*, vol. 104, no. 2, 2016.
- [6] A. Alkhachroum, K. Terilli, M. Meghani, and S. Park, "Harnessing Big Data in Neurocritical Care in the Era of Precision Medicine," 2020.
- [7] N. Gambarotta, F. Aletti, G. Baselli, and M. Ferrario, "A review of methods for the signal quality assessment to improve reliability of heart rate and blood pressures derived parameters," 2016.
- [8] J. X. Sun, A. T. Reisner, and R. G. Mark, "A signal abnormality index for arterial blood pressure waveforms," in *Computers in Cardiology*, vol. 33, 2006.
- [9] T. Edinburgh, P. Smielewski, S. Eglén, M. Czosnyka, and A. Ercole, "DeepClean - self-supervised artefact rejection for intensive care waveform data using generative deep learning," 2019.
- [10] Y. Son, S. B. Lee, H. Kim, E. S. Song, H. Huh, M. Czosnyka, and D. J. Kim, "Automated artifact elimination of physiological signals using a deep belief network: An application for continuously measured arterial blood pressure waveforms," *Information Sciences*, vol. 456, 2018.
- [11] B. Depreitere, F. Güiza, G. Van den Berghe, M. U. Schuhmann, G. Maier, I. Piper, and G. Meyfroidt, "Can optimal cerebral perfusion pressure in patients with severe traumatic brain injury be calculated based on minute-by-minute data monitoring?" *Acta Neurochirurgica, Supplementum*, vol. 122, 2016.
- [12] C. L. Tsien, I. S. Kohane, and N. McIntosh, "Building ICU artifact detection models with more data in less time." *Proceedings / AMIA ... Annual Symposium. AMIA Symposium*, 2001.
- [13] T. Lo, I. Piper, B. Depreitere, G. Meyfroidt, M. Poca, J. Sahuquillo, T. Durduran, P. Enblad, P. Nilsson, A. Ragauskas, K. Kiening, K. Morris, R. Agbeko, R. Levin, J. Weitz, C. Park, and P. Davis, "KidsBrainIT: A new multi-centre, multi-disciplinary, multi-national paediatric brain monitoring collaboration," in *Acta Neurochirurgica, Supplementum*, 2018, vol. 126.
- [14] G. Jiang, P. Xie, H. He, and J. Yan, "Wind Turbine Fault Detection Using a Denoising Autoencoder with Temporal Information," *IEEE/ASME Transactions on Mechatronics*, vol. 23, no. 1, 2018.
- [15] V. Chandola, A. Banerjee, and V. Kumar, "Anomaly detection: A survey," 2009.
- [16] I. Goodfellow, Y. Bengio, and A. Courville, *Deep learning An MIT Press Book*. MIT Press, 2016, vol. 29, no. 7553.
- [17] Y. LeCun, Y. Bengio, and G. Hinton, "Deep learning. nature 521 (7553): 436," *Nature*, vol. 521, 2015.
- [18] D. P. Kingma and M. Welling, "Auto-encoding variational bayes," in *2nd International Conference on Learning Representations, ICLR 2014 - Conference Track Proceedings*, 2014.
- [19] —, "An introduction to variational autoencoders," 2019.
- [20] I. Higgins, L. Matthey, A. Pal, C. Burgess, X. Glorot, M. Botvinick, S. Mohamed, and A. Lerchner, "B-VAE: Learning basic visual concepts with a constrained variational framework," in *5th International Conference on Learning Representations, ICLR 2017 - Conference Track Proceedings*, 2017.

This figure "fig1.png" is available in "png" format from:

<http://arxiv.org/ps/2203.05947v1>